Development/Plasticity/Repair

Motoneurons Derived from Embryonic Stem Cells Express Transcription Factors and Develop Phenotypes Characteristic of Medial Motor Column Neurons

Prabakaran Soundararajan,[1] Gareth B. Miles,[1] Lee L. Rubin,[3] Robert M. Brownstone,[1,2] and Victor F. Rafuse[1]

Departments of [1]Anatomy and Neurobiology and [2]Surgery, Dalhousie University, Halifax, Nova Scotia, Canada, B3H 1X5, and [3]Curis, Inc., Cambridge, Massachusetts 02138

Embryonic stem (ES) cells differentiate into functional motoneurons when treated with a sonic hedgehog (Shh) agonist and retinoic acid (RA). Whether ES cells can be directed to differentiate into specific subtypes of motoneurons is unknown. We treated embryoid bodies generated from HBG3 ES cells with a Shh agonist and RA for 5 d in culture to induce motoneuron differentiation. Enhanced green fluorescent protein (eGFP) expression was used to identify putative motoneurons, because eGFP is expressed under the control of the *Hb9* promoter in HBG3 cells. We found that 96 ± 0.7% of the differentiated eGFP$^+$ motoneurons expressed Lhx3, a homeobox gene expressed by postmitotic motoneurons in the medial motor column (MMC_m), when the treated cells were plated on a neurite-promoting substrate for 5 d. When the treated embryoid bodies were transplanted into stage 17 chick neural tubes, the eGFP$^+$ motoneurons migrated to the MMC_m, expressed Lhx3, projected axons to the appropriate target for MMC_m motoneurons (i.e., epaxial muscles), and contained synaptic vesicles within intramuscular axonal branches. *In ovo* and *in vitro* studies indicated that chemotropic factors emanating from the epaxial muscle and/or surrounding mesenchyme likely guide Lhx3$^+$ motoneurons to their correct target. Finally, whole-cell patch-clamp recordings of transplanted ES cell-derived motoneurons demonstrated that they received synaptic input, elicited repetitive trains of action potentials, and developed passive membrane properties that were similar to host MMC_m motoneurons. These results indicate that ES cells can be directed to form subtypes of neurons with specific phenotypic properties.

Key words: **development; sonic hedgehog; chemotropic; Lhx3; axon guidance; transcription factor; spinal cord; stem cells; regeneration; neuromuscular; motoneuron (motor neuron)**

Introduction

Neurodegenerative disorders are suited for cell replacement therapy, because they often target individual classes of neurons that are circumscribed within defined regions of the CNS. Recent research has highlighted the possible use of embryonic stem (ES) cells as sources of neurons with unlimited resource potential (Keller, 2005). It is generally accepted that ES cells must be directed to differentiate into discrete neuronal phenotypes that specifically match the properties of the degenerated neurons. However, most ES cell studies have simply classified neurons by their neurotransmitter phenotype (Bjorklund and Isacson, 2002). This classification is insufficient, because subpopulations of neurons that express a given transmitter can differ remarkably with respect to size, ion channels, receptors, projection patterns, and function. The clinical importance of these differences has recently been demonstrated in human fetal mesencephalon transplantation studies for Parkinson's disease (PD). Postmortem analysis indicated that the clinical benefit likely resulted from the selective survival and growth of a specific subtype of dopaminergic neuron located in the graft (Mendez et al., 2005). Importantly, the surviving dopaminergic neurons were the same subtype lost in PD. Therefore, for ES cells to be considered for transplantation studies, it will be necessary to direct them to differentiate into distinct neuronal subtypes with appropriate physiological properties and connections.

Neuronal differentiation results from the expression of distinct combinations of transcription factors that regulate the development of precise phenotypic traits (Jessell, 2000). For example, different subtypes of developing motoneurons innervating epaxial, hypaxial, and limb muscles express unique combinations of LIM-homeobox transcription factors (Sharma and Belmonte, 2001). These factors regulate molecules that orchestrate the lateral migration of motoneurons to specific motor columns within the developing neural tube and guide their axons to the appro-

Received Aug. 3, 2005; revised Feb. 3, 2006; accepted Feb. 3, 2006.

This work was supported by grants from the Natural Sciences and Engineering Research Council of Canada (V.F.R.), Canadian Institutes for Health Research (V.F.R.), Project A.L.S. (R.M.B.), and the Atlantic Canada Opportunities Agency through the Atlantic Innovation Fund (R.M.B.). G.B.M. is supported by a New Zealand Foundation for Research Science and Technology postdoctoral fellowship (DALH0201). P.S. is supported by a Nova Scotia Health Research Foundation scholarship. We thank Dr. Lynn Landmesser for her helpful comments during the preparation of this manuscript. The Islet-1/2, Lim1/2, and Lhx3 antibodies were obtained from the Developmental Studies Hybridoma Bank under the auspices of the National Institute of Child Health and Human Development and maintained by the University of Iowa Department of Biology. We thank Curis, Inc., for the supply of HhAg1.3 and HhAg1.4, provided under the auspices of an agreement with Project A.L.S.

Correspondence should be addressed to either Dr. Victor F. Rafuse or Dr. Robert M. Brownstone, Department of Anatomy and Neurobiology, Dalhousie University, Sir Charles Tupper Medical Building, 5850 College Street, Halifax, Nova Scotia, Canada, B3H 1X5. E-mail: vrafuse@dal.ca or rob.brownstone@dal.ca.

DOI:10.1523/JNEUROSCI.5537-05.2006

 0270-6474/06/263256-13$15.00/0

priate muscle groups (Tsuchida et al., 1994; Kania et al., 2000; Sharma et al., 2000).

ES cells differentiate into motoneurons, establish functional synapses with muscle fibers, and acquire physiological properties characteristic of embryonic motoneurons when cultured with a sonic hedgehog (Shh) agonist and retinoic acid (RA) (Wichterle et al., 2002; Harper et al., 2004; Miles et al., 2004). Interestingly, the vast majority of the Hb9$^+$ cells coexpressed Lhx3 when treated for 5 d with RA and the Shh agonist (Wichterle et al., 2002), suggesting that this treatment paradigm produces motoneurons specific to the medial aspect of the medial motor column (MMC_m). Motoneurons in the MMC_m innervate epaxial muscles (Tosney and Landmesser, 1985a,b). However, because all developing motoneurons transiently express Lhx3 (Sharma et al., 1998), it is not known whether other motoneuron phenotypes would develop if the treated cells were cultured for longer periods of time. More importantly, the functional consequence of specific LIM-homeobox gene expression patterns in ES cell-derived motoneurons is not understood.

We therefore sought to determine whether Shh agonist- and RA-treated ES cell-derived motoneurons acquire phenotypic traits specific for individual motoneuron subtypes. We found that ES cell-derived motoneurons transplanted into the developing chick neural tube expressed Lhx3, migrated to the MMC_m, projected axons toward epaxial muscles, received synaptic input, and developed electrophysiological properties similar to endogenous MMC_m motoneurons. These results indicate that Shh and RA treatment of ES cells leads to the differentiation of functional motoneurons specific to the MMC_m.

Materials and Methods

Cell culture and immunocytochemistry. The HBG3 ES cells (a kind gift provided by Dr. T. Jessell, Columbia University. New York, NY) were cultured to form embryoid bodies as described previously (Miles et al., 2004). After 2 d, the embryoid bodies were treated with a Shh agonist (Hh-Ag1.3 or Hh-Ag1.4; 1 μM; Curis, Cambridge, MA) and RA (1 μM; Sigma, St. Louis, MO), cultured as free-floating cells for an additional 5 d, after which time they were plated on coverslips coated with a neurite-promoting substrate (growth-factor reduced matrigel; BD Biosciences, Bedford, MA). One day after plating, the medium was supplemented with GDNF (glial-derived neurotrophic factor) (20 ng/ml; Upstate Biotechnology, Lake Placid, NY) and CNTF (ciliary neurotrophic factor) (10 ng/ml; Upstate Biotechnology).

Five days after plating, the cells were fixed in 3.7% paraformaldehyde for 20 min, washed three times in PBS, and incubated with either an antibody against Lim1/2 (1:2; Developmental Studies Hybridoma Bank, Iowa City, IA) or Lhx3 (1:50; Developmental Studies Hybridoma Bank) in PBS containing 10% goat serum at 4°C for 12 h. The cells were subsequently washed with PBS, incubated with a Cy3-conjugated goat anti-mouse secondary antibody (1:500; Jackson ImmunoResearch, West Grove, PA) at room temperature (RT) for 2 h, washed, and then mounted in Vectashield (Vector Laboratories, Burlington, Ontario, Canada). Images were captured using a digital camera (Nikon Coolpix 4500; Nikon, Mississauga, Ontario, Canada) mounted on a fluorescence microscope (Leica DMLFS; Leica, Richmond Hill, Ontario, Canada). The proportion of enhanced green fluorescent protein-positive (eGFP$^+$)/Lhx3$^+$ and eGFP$^+$/Lim1$^+$ cells was quantified by randomly selecting 150 eGFP$^+$ cells/well in four separate experiments. Each randomly selected cell was subsequently analyzed for Lhx3 or Lim1 expression.

In ovo *transplantations*. Fertile eggs (Truro, Nova Scotia, Canada) from white leghorn chickens (*Gallus domesticus*) were incubated at 37°C in a humidified incubator. Under sterile conditions, a window (15 × 15 mm) was made in the shell of eggs containing stage (st.) 17–18 embryos (Hamburger and Hamilton, 1951) with a dental drill. Neutral red (0.1%; Sigma) was used to aid in the visualization of the vitelline membranes, which were cut to allow access to the embryo. Using a flamed sharpened tungsten needle (0.077 mm wire) (WPI, Sarasota, FL), an incision, spanning one-somite long, was made in the dorsum of the neural tube to expose the lumen at the level of somite 26 or 27. The ependymal layer on the right side was disrupted, and a single embryoid body containing ~120 eGFP$^+$ cells was transplanted into the ventral region of the neural tube. This graft location reproducibly ensured that the eGFP$^+$ cells were located in LS1 and/or LS2. The number of eGFP$^+$ cells in a single embryoid body was estimated as described by Martin et al. (1997). Ten or 275 eGFP$^+$ cells were transplanted into the neural tube in a few noted studies. In addition, the embryoid body was deliberately placed in the dorsal region of the neural tube in one set of experiments. The eggs were then sealed and incubated until st. 25, 31, 36, 38, or 40.

Posttransplant eGFP$^+$ cell quantification and immunohistochemistry. Control and transplanted embryos were quickly killed by decapitation. The embryos were fixed in 4% formaldehyde for 1 h at RT, washed three times in cold (4°C) PBS, and left in PBS overnight at 4°C. The embryos were incubated in 30% sucrose/PBS for 2 h at 4°C, mounted in Tissue Tek (Sakura Finetek, Torrance, CA), and stored at −80°C. Coronal sections (30 μm) were cut using a cryostat, dried on superfrost slides, and mounted in Vectashield (Vector Laboratories). The total number of eGFP$^+$ cells in all of the sections was counted, and the raw counts were corrected via the method described by Abercrombie (1946).

For immunohistochemical analysis, the sections were washed for 20 min in PBS and incubated overnight at 4°C with primary antibodies. The following primary antibodies were used: Lim1/2 (1:2), Lhx3 (1:50), SV2 (1:2) (all from Developmental Studies Hybridoma Bank), β-III tubulin (1:5000; Covance Research Products, Princeton, NJ), and a polyclonal EphA4 antibody (1:1000; a kind gift provided by Dr. David Wilkinson, National Institute for Medical Research, London, UK). The sections were washed, incubated with either a goat anti-mouse or goat anti-rabbit secondary antibody (1:500; Cy2 or Cy3; Jackson ImmunoResearch) at RT for 2 h, washed in PBS, and finally mounted in Vectashield (Vector Laboratories). The location and projection patterns of all of the eGFP$^+$ motoneurons transplanted into single embryos were reconstructed from coronal sections using Neurolucida software (MicroBrightField, Williston, VT).

In ovo *Lhx3$^+$ motoneuron quantification.* The total number of MMC_m Lhx3$^+$ neurons (left and right side counted separately) was quantified from sections of the neural tube that spanned 200 μm rostral and caudal to the epicenter of the graft (i.e., 400 μm in total). Each section was processed for Lhx3 immunohistochemistry (method described above) and Hoechst nuclear stain (Sigma). The double staining was used because Lhx3 is a nuclear transcription factor, whereas eGFP is expressed in both the nucleus and cytoplasm. The total number of Lhx3$^+$ cells in the MMC_ms on both sides was counted, and the raw counts were corrected via the method described by Abercrombie (1946). Statistical analysis of the two sides was performed using Student's *t* test.

Retrograde labeling of motoneurons. St. 35–36 control and transplanted chick embryos were quickly killed by decapitation and eviscerated, skin was removed, and a ventral laminectomy was performed in cold, well oxygenated Tyrode's. The longissimus, sartorius, or femorotibialis muscle was injected with 1% Alexa Fluor 594-conjugated cholera toxin B (CTb) (Molecular Probes, Eugene, OR), and the embryos were quickly placed in well oxygenated Tyrode's maintained at 33°C for 4 h. The embryos were either fixed immediately in 4% paraformaldehyde or used in whole-cell patch-clamp recordings (described below).

Embryoid body/muscle explant cocultures. Longissimus (epaxial) and caudilioflexorius (limb) muscle fibers were isolated from st. 35 chick embryos. Hh-Ag1.3/RA-treated embryoid bodies (5 d treatment) were flanked by the longissimus and caudilioflexorius muscle fibers in three-dimensional (3-D) collagen gels (rat tail type I collagen; BD Biosciences) (Guthrie and Lumsden, 1994). The cells were fixed 18 h later and imaged with a Zeiss LSM confocal microscope. Images were acquired every 3.87 μm along the entire *z*-axis of the embryoid body. The number of neurites extending toward the two muscles was quantified on-line from the confocal images. Neurite location was scored as being either in the proximal hemisphere closest to the muscle fiber explant or in the distal hemisphere furthest away. This imaging and counting technique ensured that all of

the neurites extending from the embryoid bodies were included in the quantitative analysis.

Slice preparation. Electrophysiological experiments were performed on acute spinal cord slices obtained from stage 31–36 chick embryos. Chick embryos were decapitated and eviscerated, and the spinal cord was dissected free in cold (<4°C) artificial CSF. The lumbar enlargement was isolated, placed in a 1% agar solution, mounted in a vibrating microtome (Vibratome 3000; Vibratome, St. Louis, MO), and sliced (250 μm) using a sapphire blade (Delaware Diamond Knives, Wilmington, DE). Slices were immediately transferred to a holding chamber containing recording Tyrode's solution at RT (22–24°C). Individual slices were then transferred to a recording chamber (Warner Instruments, Hamden, CT) that was continuously perfused (3–5 ml/min) with recording Tyrode's solution at RT, where they were visualized with epifluorescence and infrared differential interference contrast (IR-DIC) microscopy using a Leica DMLFSA upright microscope (Leica) and a DAGE IR-1000 digital camera (DAGE-MTI, Michigan City, IN).

Whole-cell patch-clamp recordings. Whole-cell patch-clamp recordings were made from eGFP$^+$ ES cell-derived motoneurons or endogenous chick motoneurons backlabeled with 1% Alexa Fluor 594-conjugated CTb (Molecular Probes). Signals recorded using whole-cell patch-clamp techniques were recorded with a MultiClamp 700B amplifier (Molecular Devices, Union City, CA), acquired at ≥10 kHz using a Digidata 1322A and pClamp software (Molecular Devices). Series resistance was monitored and compensated at least 60%. Whole-cell capacitance, and input resistance values were calculated using pClamp software. All voltage- and current-clamp protocols are described in Results. Signals were analyzed off-line using Clampfit software (Molecular Devices).

Solutions. The dissecting artificial CSF was sucrose based and contained (in mM): 25 NaCl, 188 sucrose, 1.9 KCl, 10 $MgSO_4$, 26 $NaHCO_3$, 1.2 NaH_2PO_4, 25 D-glucose, 1.5 kynurenic acid (equilibrated with 95% O_2/5% CO_2). The recording Tyrode's solution contained (in mM): 139 NaCl, 2.9 KCl, 3 $CaCl_2$, 1 $MgCl_2$, 17 $NaHCO_3$, 12.2 D-glucose (equilibrated with 95% O_2/5% CO_2). The pipette solution for whole-cell patch-clamp recordings contained (in mM): 140 potassium methane-sulfonate, 10 NaCl, 1 $CaCl_2$, 10 HEPES, 1 EGTA, 3 ATP-Mg, 0.4 GTP (pH 7.2–7.3, adjusted with KOH).

Statistical analysis. Mean values (±SEMs) are shown throughout. Student's *t* test was used to compare means from different experimental groups.

Results

We treated embryoid bodies generated from HBG3 cells with RA and the Shh agonist Hh-Ag1.3, or Hh-Ag1.4, for 5 d in culture, as described by Wichterle et al. (2002) (see also Miles et al., 2004). Because no notable differences were observed between the two agonists, we simply refer to the two compounds as Hh-Ag1.3 throughout the paper for simplicity. Enhanced GFP is expressed under the control of the mouse HB9 promoter (Wichterle et al., 2002) in HBG3 cells, and thus eGFP expression can be used to identify putative motoneurons (Wichterle et al., 2002; Harper et al., 2004; Miles et al., 2004). The treated embryoid bodies were subsequently plated on coverslips and cultured for an additional 5 d. Figure 1 shows that the majority of eGFP$^+$ cells had extensive neurites 5 d after plating. Interestingly, although Lim1$^+$ neurons were present in the cultures (Fig. 1*A*, arrowhead), the vast majority of them were not eGFP$^+$ and thus likely represented V0 and/or V1 interneurons (Ericson et al., 1997a,b). Only 4.49 ± 0.706% of the eGFP$^+$ neurons in four separate experiments expressed Lim1 5 d after plating. In contrast, almost all of the plated eGFP$^+$ neurons expressed Lhx3 (96.1 ± 0.702%; $n = 4$) 5 d after plating (Fig. 1*B*). Together with the study of Wichterle et al. (2002), these results indicate that the expression of Lhx3 in ES cell-derived motoneurons is not transient and that RA- and Hh-Ag1.3-treated ES cells appear to establish a Lhx3$^+$ MMC_m motoneuron identity.

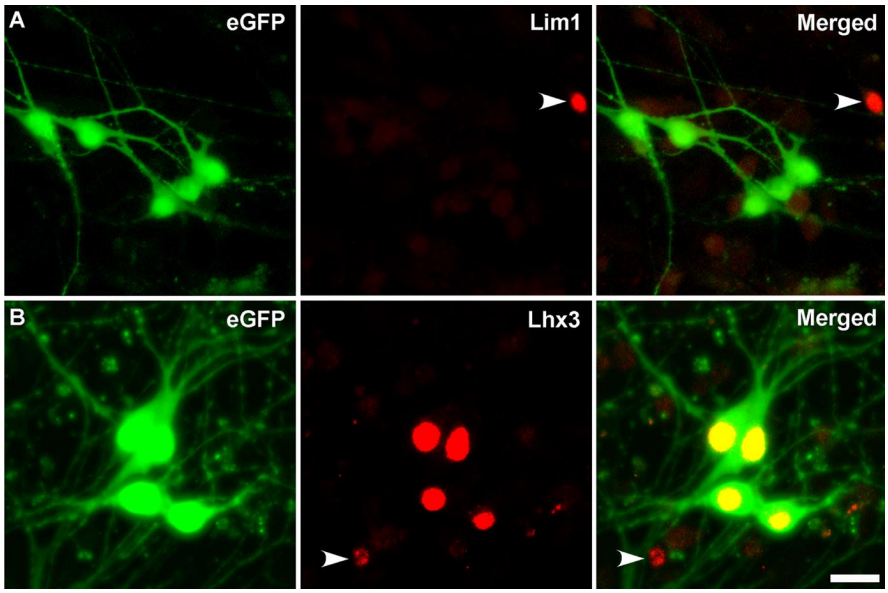

Figure 1. ES cell-derived motoneurons continually express Lhx3 in culture when previously exposed to RA and Hh-Ag1.3. ***A***, ***B***, The majority of eGFP$^+$ cells had extensive neurites 5 d after plating. ***A***, Immunolabeling showed that very few of the eGFP$^+$ ES cell-derived motoneurons expressed Lim1, although eGFP$^-$/Lim1$^+$ cells were occasionally observed (***A***, arrowhead). ***B***, In contrast, the vast majority of the eGFP$^+$ cells, and a few eGFP$^-$ cells (***B***, arrowhead), expressed Lhx3. Scale bar, 20 μm.

Lhx3 regulates migration and axon targeting

To determine whether the migration and axon targeting of ES cell-derived motoneurons is appropriate for HB9/Lhx3-expressing cells, we transplanted Hh-Ag1.3/RA-treated embryoid bodies containing ~120 eGFP$^+$ cells into the neural tube lumen of st. 17 chick embryos (for details, see Materials and Methods). Care was taken to place the embryoid bodies in the ventral one-half of the neural tube where motoneuron neurogenesis normally occurs (Hollyday and Hamburger, 1977). The Hh-Ag1.3/RA-treated embryoid bodies were always transplanted into the neural tube at the level of somite 26 or 27. This graft location ensured that the eGFP$^+$ cells translocated into the LS1 and/or LS2 region of the spinal cord. In the first set of experiments, the embryos were allowed to develop until st. 31, after which time they were processed for immunohistochemistry. The majority (80.1 ± 0.352%; 235 cells counted in three embryos) of the transplanted ES cell-derived motoneurons migrated through the ependymal layer to reside within the medial one-third of the MMC_m (Fig. 2*A*,*C*). The vast majority of the eGFP$^+$ cells that did not migrate to the MMC were located dorsal to the motor column in the ventral one-half of the neural tube (Figs. 3*D*, 8*B*).

Both low- (Fig. 2*A*) and high-magnification (Fig. 2*B*) confocal microscopy revealed that the transplanted ES cell-derived motoneurons did not express Lim1 at st. 31. Although less intensely stained than the endogenous chick Lhx3$^+$ neurons (Fig. 2*C*), high-magnification confocal microscopy clearly showed that the transplanted ES cell-derived motoneurons expressed Lhx3 (Fig.

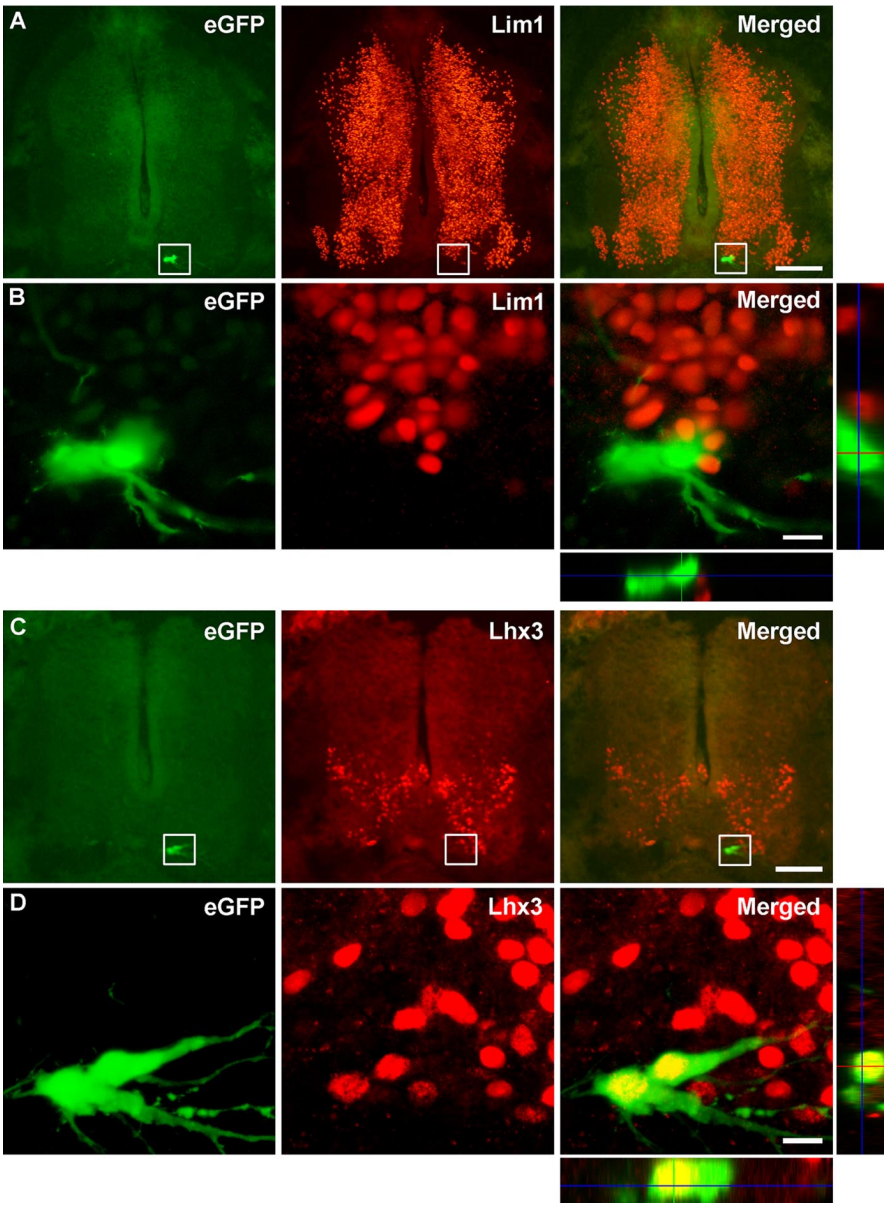

Figure 2. ES cell-derived motoneurons translocate to the MMC_m and continue to express Lhx3 when transplanted *in ovo*. ***A***, ***C***, Cross sections through st. 31 chick embryos showed that the majority of the transplanted $eGFP^+$ cells translocated to the medial/ventral aspect of the developing neural tube. ***A***, ***B***, Immunolabeling and confocal imaging showed that none of the transplanted $eGFP^+$ cells were $Lim1^+$. ***B***, Images are a higher magnification of the corresponding boxes shown in ***A***. Imaging in both the *x–z* and *y–z* orthogonal planes confirm that the $eGFP^+$ cells were $Lim1^-$. ***C***, ***D***, Although less intensely stained than the endogenous chick $Lhx3^+$ neurons, all of the transplanted $eGFP^+$ cells were $Lhx3^+$. ***D***, Images are a higher magnification of the boxes shown in ***C***. Imaging in both the *x–z* and *y–z* orthogonal planes confirms the expression of Lhx3 in $eGFP^+$ cells (***D***). In all sections, dorsal is up. Scale bars: ***A***, ***C***, 250 μm; ***B***, ***D***, 20 μm.

2*D*). To quantify the number of $eGFP^+/Lhx3^+$ cells, we examined Lhx3 expression in all of the $eGFP^+$ cells in three st. 31 embryos. One hundred percent of the $eGFP^+$ cells in the three embryos examined (282 cells counted) expressed Lhx3.

To determine whether the number of endogenous motoneurons was altered in the transplanted embryos, we counted all of the MMC_m $Lhx3^+/eGFP^-$ cells in a section of the neural tube that spanned 200 μm rostral and caudal to the epicenter of the graft (three embryos examined). Because the ependymal layer was not disrupted on the left side, and because the vast majority of the transplanted cells migrated into the right side of the neural tube (Fig. 2), we reasoned that the graft would not affect the number of endogenous $Lhx3^+$ MMC_m motoneurons on the left side. The numbers of $Lhx3^+/eGFP^-$ cells in the right (mean ± SEM, 356 ± 32.3) and left (376 ± 74.4) MMC_ms were not significantly different from each other ($p = 2.78$). Consequently, the number of endogenous MMC_m motoneurons ipsilateral to the graft was not altered by the transplantation. This conclusion is supported by immunohistochemical studies that show that the distribution and number of $Lim1^+$ and $Lhx3^+$ cells were not visibly different on the two sides of the neural tube (Fig. 2).

To ascertain whether $Lhx3^+$ ES cell-derived motoneurons appropriately target epaxial muscles, we transplanted ~120 $eGFP^+$ cells into the neural tube of st. 17 chick embryos. The embryos were allowed to develop until st. 31, after which time they were immunolabeled with β-III tubulin to visualize both endogenous chick and transplanted mouse neurons. As expected from Wichterle et al. (2002), the $eGFP^+$ motoneurons extended axons out of the neural tube through the ventral root (Fig. 3*B*, arrow). However, in contrast to Wichterle et al. (2002) (see below), all of the $eGFP^+$ axons in our study ($n = 12$ of 12 embryos) grew around the dorsal root ganglion (DRG) (Fig. 3*A*,*B*, arrowheads), extended dorsally as part of the dorsal ramus (Fig. 3*C*, arrow) where they either innervated the longissimus muscle (Fig. 3*C*, arrowheads) or skin (see below). Neurolucida reconstruction of one representative st. 31 chick embryo unequivocally demonstrated that all of the $eGFP^+$ axons (Fig. 3*D*, green tracings) projected dorsally where they either formed part of the longissimus muscle nerve (Fig. 3*D*, arrow) or misprojected to the skin along the endogenous cutaneous nerve (Fig. 3*D*, arrowhead). Together, these results indicate that $Lhx3^+$ ES cell-derived motoneurons do not passively extend axons along major nerve pathways that lead to different muscle groups in the body wall and limbs, but rather selectively project axons to dorsal targets innervated by the dorsal ramus. However, unlike $Lhx3^+$ MMC_m motoneurons, several of the ES cell-derived motoneurons incorrectly projected to the skin at the junction where the dorsal ramus bifurcates into the longissimus muscle branch and cutaneous nerve (see below and Discussion).

Transplanted ES cell-derived motoneurons survive beyond the cell death period

The number of $eGFP^+$ cells in the neural tube was determined before, during, and after the naturally occurring cell death period to characterize the degree and pattern of cell survival (Fig. 4*A*). We estimated that the transplanted embryoid bodies contained ~120 $eGFP^+$ cells from the technique described by Martin et al.

(1997). Before the cell death period (st. 25), the neural tubes contained 109 ± 7.50 cells. This number decreased to 81.1 ± 5.33 and 22.6 ± 7.64 cells by st. 31 and 36, respectively. The number of eGFP$^+$ cells continued to decrease until after the cell death period (st. 38), at which it remained stable at ~10 cells for at least 2 more days.

The temporal pattern of eGFP$^+$ cell death was remarkably similar to the normal time course in naturally occurring cell death (Hamburger, 1975; Tanaka and Landmesser, 1986). However, the extent of cell death was greater than the usual 50% loss in motoneurons. The greater cell death is attributable, at least in part, to the fact that approximately one-half of the eGFP$^+$ cells misprojected axons to the skin (Fig. 3) (see below). All of the transplanted motoneurons extending to the skin presumably died by st. 38, because eGFP$^+$ axons were not observed projecting to the skin after st. 36 (data not shown). However, if one-half of the transplanted motoneurons died by naturally occurring cell death, and another 50% died because they misprojected to the skin, then the final number of surviving eGFP$^+$ motoneurons should be ~30 rather than the observed 10. Consequently, other factors must be responsible for the higher than expected cell death. The most likely possibility is that some of the ES cell-derived neurons were "outcompeted" by the endogenous motoneurons during the process of cell death. Another possibility is that some of the eGFP$^+$ motor axons projecting to the longissimus died because they did not actually innervated the muscle. To determine how many ES cell-derived motoneurons innervated their correct target, we injected a retrograde tracer (CTb) into the longissimus muscle of three st. 35 embryos. Both endogenous and ES cell-derived motoneurons innervating the longissimus muscle accumulated CTb in their cell bodies (Fig. 4*B*,*C*). Quantitative analysis indicated that 49% (ranged from 30 to 67%) of the eGFP$^+$ motoneurons innervated the longissimus muscle at st. 35. It should be noted, however, that it is highly unlikely that 100% of the innervating eGFP$^+$ neurons were backlabeled, because intramuscular injections of retrograde tracers label a variable number (25–90%) of innervating motoneurons (Dasen et al., 2005). Thus, we can only conclude that 30–67% of the ES cell-derived motoneurons innervated the longissimus muscle by st. 35. Those that did not likely died because of a lack of trophic support (Hamburger, 1958; Oppenheim et al., 1978). We did not determine how many ES cell-derived motoneurons innervated the longissimus muscle at earlier stages, because the very thin architecture of the muscle precluded reliable intramuscular labeling of the innervating motoneurons.

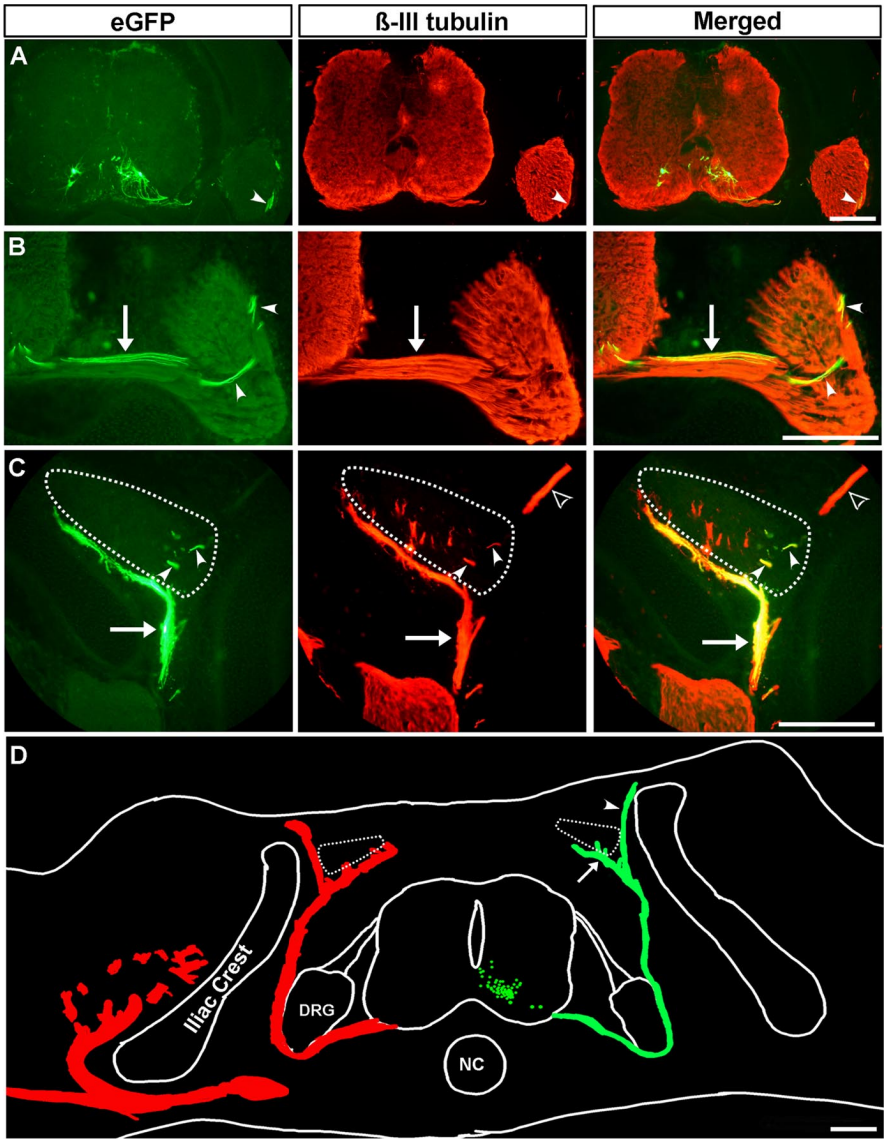

Figure 3. Transplanted ES cell-derived motoneurons project axons to axial muscles. ***A***, ***D***, Cross sections through st. 31 chick embryos showed that the majority of the transplanted eGFP$^+$ cells translocated to the medial/ventral aspect of the neural tube. ***B***, ES cell-derived motoneurons extended axons out of the neural tube through the ventral root (***B***, arrow) and projected dorsally around the DRG as part of the dorsal ramus (***A***, ***B***, arrowheads). ***C***, Dorsal projecting eGFP$^+$ axons formed part of the dorsal ramus (***C***, arrow) and innervated the longissimus muscle (***C***, arrowheads; muscle delineated by dotted line). The endogenous cutaneous nerve is indicated with an open arrowhead. ***A–C***, β-III tubulin immunohistochemistry was used to visualize both the endogenous chick and transplanted mouse neurons. ***D***, Neurolucida reconstruction shows that all of the eGFP$^+$ axons in a representative st. 31 chick embryo (green tracings) projected dorsally and either formed part of the longissimus muscle nerve (***D***, arrow) or incorrectly targeted the skin (***D***, arrowhead). Each green dot in the neural tube represents one eGFP$^+$ neuron. For comparison, the projection patterns of the endogenous β-III tubulin$^+$ chick neurons are shown in red on the contralateral side. The longissimus muscles are indicated with dotted lines. In all sections, dorsal is up. NC, Notochord. Scale bars: ***A***, ***D***, 100 μm; ***B***, ***C***, 200 μm.

To determine whether ES cell-derived motoneurons expressed presynaptic proteins required for synapse formation, we immunolabeled transplanted chick embryos with a synaptic vesicle specific antibody (SV2) at st. 35. Confocal imaging showed that the distribution of synaptic vesicles in the endogenous chick axons (Fig. 4*D*, arrowheads) and eGFP$^+$ axons (Fig. 4*D*, arrows) was the same. This distribution is consistent with previous studies in both chick (Dahm and Landmesser, 1991) and mice (Lupa and Hall, 1989) showing that synaptic vesicles are distributed along the entire length of developing muscle nerves including intramuscular nerve branches.

Together, these results indicate that transplanted Hh-Ag1.3/RA-treated embryoid bodies specifically migrate to the MMC_m [i.e., not the lateral motor column (LMC)], project dorsally as

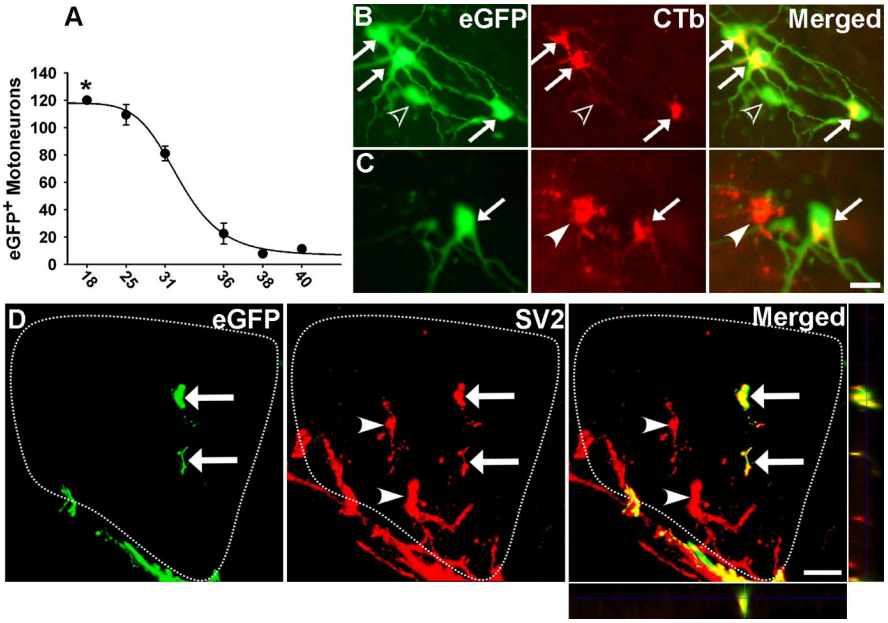

Figure 4. Transplanted ES cell-derived motoneurons survive beyond the cell death period, innervate the epaxial muscle, and express presynaptic proteins required for synapse formation. ***A***, The number of eGFP $^{+}$ cells in the neural tube was quantified before (st. 25), during (st. 31 and 36), and after (st. 38 and 40) the naturally occurring cell death period to characterize the degree and pattern of cell survival. The asterisk denotes that the cell number was an estimate. The curve was fitted according to the formula: $y = \min + (\max - \min)/(1 + (x/EC_{50})^{HillSlope})$ and had an r^2 value of 0.998. Error bars indicate SE. ***B***, ***C***, Cross sections through the MMC_m shows eGFP $^{+}$ cell bodies that either contained (arrows) or did not contain (open arrowhead) the retrograde tracer CTb. A backlabeled endogenous MMC_m neuron is also present (***C***, arrowhead). ***D***, Confocal imaging shows that the eGFP $^{+}$ axons innervating the longissimus muscle (outlined by dotted line) were immunolabeled with a synaptic vesicle-specific antibody (SV2; arrows). Endogenous eGFP $^{-}$ chick neurons are indicated with arrowheads. Imaging in both the *x–z* and *y–z* orthogonal planes confirm that the eGFP $^{+}$ axons were SV2 $^{+}$. Scale bars: (in ***C***) ***B***, ***C***, 30 μm; ***D***, 20 μm.

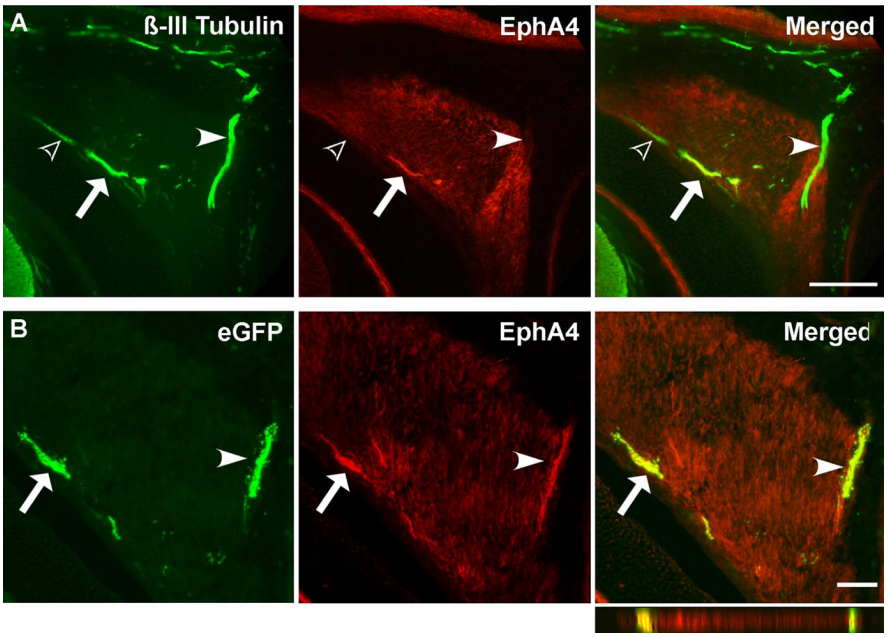

Figure 5. Transplanted ES cell-derived motoneurons express guidance molecules appropriate for MMC_m motoneurons. ***A***, Cross section shows that the axon shaft (arrow), but not the distal tips (open arrowhead), of β-III tubulin $^{+}$ neurons projecting along the ventral edge of the longissimus muscle expressed EphA4 in control st. 31 chick embryos. As expected, the cutaneous axons projecting to the skin were EphA4 $^{-}$ (arrowhead). ***B***, Confocal imaging shows that the eGFP $^{+}$ axons from the transplanted ES cell-derived motoneurons expressed EphA4 as they correctly projected along the ventral border of the longissimus muscle (arrow) and incorrectly projected to the skin (arrowhead). Imaging in the *x–z* orthogonal plane confirms that the eGFP $^{+}$ axons were EphA4 $^{+}$. Scale bar, 100 μm.

part of the dorsal ramus, innervate their correct muscle target, survive beyond the cell death period, and express presynaptic proteins required for synapse formation.

ES cell-derived motoneurons express appropriate guidance molecules

Previous studies indicated that chick MMC_m motoneurons express EphA4 (Eberhart et al., 2004) when targeting the epaxial muscles during embryonic development. Furthermore, attractive signaling between EphA4-expressing MMC_m motoneurons and ephrin-A5 $^{+}$ cells in the sclerotome is believed to selectively direct MMC_m axons dorsally to form part of the dorsal ramus (Eberhart et al., 2004). It therefore seemed reasonable to determine whether the axons of the transplanted ES cell-derived motoneurons expressed EphA4. We first immunolabeled control st. 31 chick embryos with anti-EphA4 and anti-β-III tubulin to visualize the expression of EphA4 on the motor and cutaneous axons innervating the longissimus muscle and overlying skin. As shown in Figure 5*A*, the axon shaft (Fig. 5*A*, long arrow), but not the distal tips (Fig. 5*A*, open arrowhead) of the MMC_m motor axons expressed EphA4 as they projected along the ventral border of the longissimus muscle. These results are similar to the differential expression of EphA4 on the axon shafts and growing tips of chick MMC_m axons reported by Eberhart et al. (2004). As expected, the cutaneous axons projecting to the skin did not express EphA4 (Fig. 5*A*, arrowhead). In the transplanted embryos, confocal imaging revealed that the eGFP $^{+}$ axons of ES cell-derived motoneurons expressed EphA4 as they projected along the ventral edge of the longissimus muscle in st. 31 chick embryos (Fig. 5*B*, arrow). Interestingly, EphA4 was also expressed on the eGFP $^{+}$ motor axons that incorrectly projected to the skin as part of the cutaneous nerve (Fig. 5*B*, arrowhead). These results indicate that ES cell-derived motoneurons express guidance molecules appropriate for MMC_m neurons.

Chemotropic mechanisms selectively guide ES cell-derived motor axons to their correct target

Developing neurons use both long- and short-range guidance molecules to selectively innervate their correct target (for review, see Landmesser, 1992; Tessier-Lavigne and Goodman, 1996; Chisholm and Tessier-Lavigne, 1999). Consequently, ES cell-derived motoneurons could selectively target epaxial muscles, because specific axon–axon adhesive in-

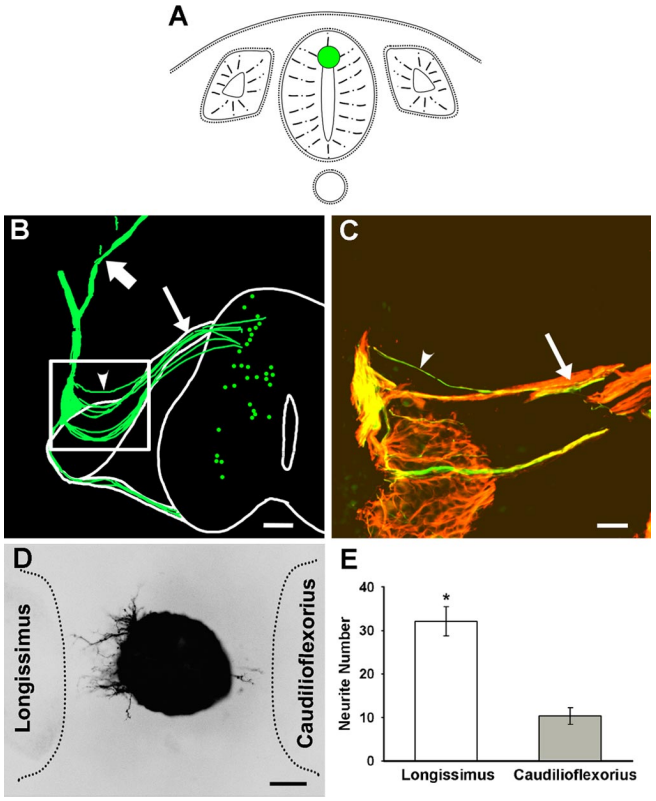

Figure 6. Chemotropic mechanisms selectively guide ES cell-derived motor axons to their correct target. ***A***, Cartoon showing the location of the Hh-Ag1.3-treated embryoid bodies that were deliberately transplanted into the dorsal hemisphere of st. 17 chick neural tubes. ***B***, Neurolucida reconstruction shows that the transplanted ES cell-derived motoneurons were primarily located in the dorsal one-half of the neural tube in a st. 31 chick embryo (green dots). The eGFP$^+$ axons (green tracings) extended out of the neural tube along the dorsal root (long arrow) where they later projected dorsally as part of the dorsal ramus. The dorsal projecting eGFP$^+$ axons later bifurcated to either form part of the longissimus muscle nerve (short arrow) or cutaneous nerve that innervates the skin. ***C***, Higher magnification of the box shown in ***B*** immunolabeled with β-III tubulin (red). eGFP$^+$/β-III tubulin$^+$ axons appear yellow in this merged image. Arrowhead shows an eGFP$^+$ axon extending away from the endogenous chick dorsal root axons. ***D***, A *z*-stack collapsed confocal image of an Hh-Ag1.3/RA-treated embryoid body that was flanked with explants harvested from the longissimus and caudilioflexorius muscles showing that the neurite outgrowth was substantially greater on the side of the longissimus muscle. The picture is shown as an inverted black and white image of the green fluorescence. Scale bars, 100 μm. ***E***, Quantitative analysis indicates that significantly more neurites grew toward the longissimus muscle explant compared with the caudilioflexorius explant ($n = 8$; *$p = 0.0004$). Error bars indicate SE.

teractions cause them to preferentially adhere to, and grow with, the endogenous chick Lhx3$^+$ MMC$_m$ motoneurons. Alternatively, they could target the epaxial muscles, because the muscle provides chemotropic signals that selectively attract Lhx3$^+$ neurons. To distinguish between these two possibilities, we deliberately transplanted ES cell-derived motoneurons into the dorsal one-half of the neural tube (st. 17–18) where neurogenesis of motoneurons does not take place (Fig. 6*A*). The embryos were allowed to develop until st. 31 when they were processed for β-III tubulin immunohistochemistry. Neurolucida reconstruction showed that many of the transplanted eGFP$^+$ motoneurons migrated through the ependymal layer to reside within the mantel layer in the dorsal one-half of the developing spinal cord (Fig. 6*B*, green dots). The ectopically located ES cell-derived motoneurons extended aberrant axonal projections out of the neural tube through the dorsal root (Fig. 6*B*,*C*, arrows). Interestingly, despite the initial anomalous projections, the eGFP$^+$ motor axons still extended dorsally at the lateral edge of the developing DRG (Fig. 6*B*,*C*) to become contiguous with the endogenous chick MMC$_m$ motoneurons that formed the dorsal ramus. Occasionally, individual eGFP$^+$ axons branched from the dorsal root and projected dorsally before reaching the DRG (Fig. 6*B*,*C*, arrowhead). These results suggest that the ES cell-derived motoneurons were not simply extending axons along previously established nerve pathways containing Lhx3$^+$ axons, but rather were selectively responding to chemotropic signals emanating from the developing epaxial muscle and/or surrounding mesenchyme. As observed with the ventrally transplanted ES cell-derived motoneurons, many of the eGFP axons correctly innervated the longissimus muscle (Fig. 6*B*, short arrow), whereas others incorrectly extended along the cutaneous nerve projecting to the skin (Fig. 6*B*) (see below and Discussion).

To further investigate whether developing epaxial muscle fibers, and/or surrounding mesenchyme, secrete diffusible factors that guide Lhx3$^+$ ES cell-derived motor axons to their correct target, we flanked Hh-Ag1.3/RA-treated embryoid bodies with st. 35 longissimus (epaxial) and caudilioflexorius (limb) muscle fibers in 3-D collagen gels. Eighteen hours later, the cells were fixed and imaged with a confocal microscope. Images were acquired every 3.87 μm along the entire *z*-axis of the embryoid body. A collapsed image of the *z*-stack from a representative experiment (Fig. 6*D*) shows that the outgrowth of neurites from the embryoid body was substantially greater on the side facing the longissimus muscle. The number of neurites extending toward the two muscles was quantified on-line from the confocal images to ensure that all of the neurites extending from the embryoid bodies were included in the quantitative analysis. Figure 6*E* shows that significantly more neurites grew toward the longissimus muscle explant compared with the caudilioflexorius explant ($n = 8$; $p = 0.00044$). Together, these results indicate that chemotropic factors emanating from the epaxial muscle, and/or surrounding mesenchyme, likely guide Lhx3$^+$ ES cell-derived motoneurons to their appropriate target.

Transplanted ES cell-derived motoneurons develop physiological properties similar to endogenous MMC$_m$ neurons

Previous studies in our lab showed that eGFP$^+$ neurons in Hh-Ag1.3/RA-treated embryoid bodies develop electrophysiological properties necessary to produce patterns of action potential firing that are appropriate for motoneurons (Miles et al., 2004). To assess whether ES cell-derived motoneurons develop functional properties expected of motoneurons when transplanted *in ovo*, we transplanted ~120 eGFP$^+$ neurons into st. 17 chick embryos. The embryos were allowed to develop until at least st. 31 when the spinal cords were harvested for whole-cell patch-clamp recordings. IR-DIC/epifluorescence microscopy was used to identify eGFP$^+$ ES cell-derived motoneurons (Fig. 7*Ai*).

Recordings were initially performed in voltage-clamp mode to determine whether ES cell-derived motoneurons express some basic voltage-activated ion channels. Using voltage steps from a holding potential of −60 mV to a range of test potentials between −60 and +20 mV (2.5 mV increments; 10 ms duration), we demonstrated that ES cell-derived motoneurons express large transient inward currents, likely fast inactivating Na$^+$ currents, and sustained outward currents, likely delayed rectifier-type K$^+$ currents (Fig. 7*Aii*) ($n = 12$).

Next, recordings were performed in current-clamp mode to determine whether ES cell-derived motoneurons could produce repetitive firing. In response to the injection of square current

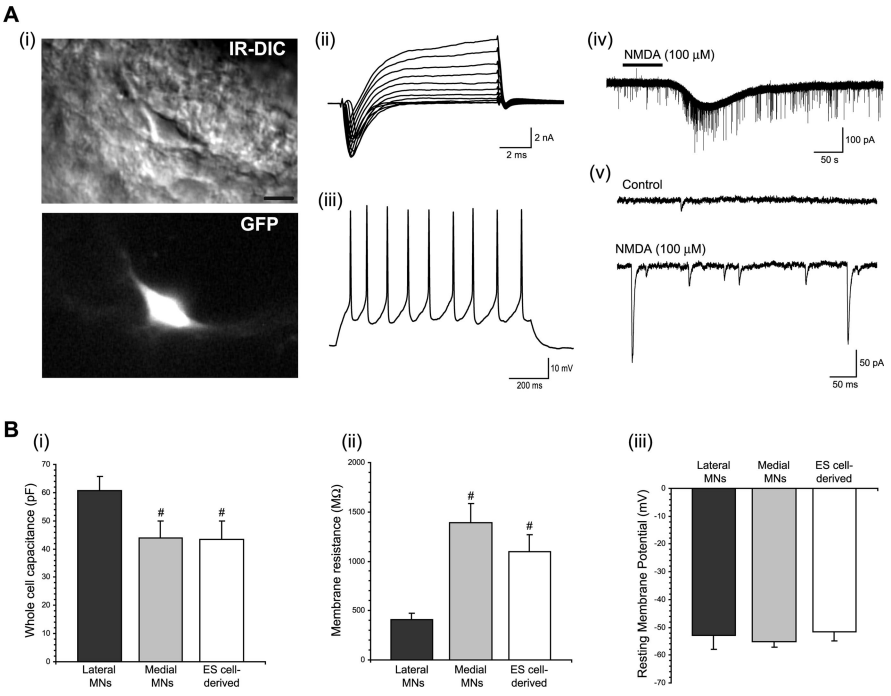

Figure 7. ES cell-derived motoneurons transplanted into the developing chick spinal cord express appropriate electrophysiological properties. ***Ai***, An ES cell-derived motoneuron in a chick spinal cord slice visualized using IR-DIC microscopy (top) and epifluorescence exciting GFP (bottom). Scale bar, 10 μm. ***Aii***, A voltage-clamp recording from an ES cell-derived motoneuron showing fast, inactivating inward currents and persistent outward currents in response to depolarizing voltage steps from a holding potential of −60 mV. ***Aiii***, A current-clamp recording from an ES cell-derived motoneuron showing repetitive firing of action potentials in response to the injection of a 1 s current pulse. ***Aiv***, A voltage-clamp recording of an ES cell-derived motoneuron held at −60 mV showing an inward current in response to the application of NMDA (100 μM). ***Av***, Recordings in ***Aiv*** shown on a faster time scale demonstrating the presence of EPSCs in control conditions and during the application of NMDA. ***Bi–Biii***, Graphs comparing the passive membrane properties of endogenous lateral and medial motoneurons (MNs) and transplanted ES cell-derived motoneurons. The pound sign indicates significant difference compared with lateral motoneuron. Error bars indicate SE.

pulses (1 s duration), 9 of 15 transplanted ES cell-derived motoneurons fired repetitive trains of action potentials (Fig. 7*Aiii*). The remaining six cells fired one to three action potentials in response to sustained current injection. The minimum current required to elicit repetitive firing in six stable cells equaled 15 ± 2 pA. Plots of steady-state firing frequency (averaged over the last 500 ms of pulses) versus injected current demonstrated that firing frequencies increased with increased current injection ($n = 6$). The average slope of *f–I* relationships was 300 ± 70 Hz/nA. The maximum rate of firing observed in cells that appeared to be driven near maximally was 16 ± 0.7 Hz ($n = 6$). These data indicate that ES cell-derived motoneurons express the cellular machinery required to produce output appropriate for motoneurons.

Next, we investigated whether ES cell-derived motoneurons were able to receive synaptic inputs after transplantation. To assess whether ES cell-derived motoneurons expressed functional glutamatergic receptors, we applied NMDA (100 μM) directly to the perfusate during voltage-clamp recordings of individual ES cell-derived motoneurons. Application of NMDA was associated with sustained inward currents (Fig. 7*Aiv*) ($n = 4$). When voltage-clamp recordings were examined on a faster time scale, EPSCs were observed in control conditions and to a greater extent when NMDA was present in the bath (Fig. 7*Av*). These data indicate that ES cell-derived motoneurons express functional NMDA receptors and can receive synaptic input after transplantation into the chick spinal cord.

Given that our *in vitro* and *in ovo* anatomical data indicate that ES cell-derived motoneurons develop a medial motoneuron identity, we proceeded to investigate (1) whether medial motoneurons have distinct electrophysiological properties and (2) whether ES cell-derived motoneurons develop these properties. To address this, we first had to compare the properties of endogenous medial and lateral motoneurons. Stage 35 or 36 chick embryos received injections of CTb into the longissimus or limb muscles to label motoneurons in the MMC_m and LMC, respectively. Whole-cell recordings were then established from medial ($n = 9$) and lateral ($n = 13$) motoneurons identified by retrograde labeling. At this developmental stage, the whole-cell capacitance of lateral motoneurons (61 ± 5 pF) was significantly greater than that of medial MNs (44 ± 6 pF; $p = 0.04$) (Fig. 7*Bi*). The membrane resistance of medial motoneurons (1390 ± 190 MΩ) was significantly greater than that of lateral motoneurons (410 ± 65 MΩ; $p < 0.0001$) (Fig. 7*Bii*). These differences are consistent with medial motoneurons being smaller neurons. In addition, because the differences in whole-cell capacitance and membrane resistance were not proportional, membrane time constants were much larger in medial (61 ms) versus lateral (25 ms) motoneurons. Such differences in membrane time constants will greatly affect synaptic integration. Data obtained from endogenous motoneurons were then compared with those of transplanted ES cell-derived motoneurons from stage 35 or 36 chick embryos. Passive membrane properties of ES cell-derived motoneurons most closely matched those of medial motoneurons. The average whole-cell capacitance of ES cell-derived motoneurons (43 ± 7 pF) (Fig. 7*Bi*) ($n = 10$) was not significantly different from the chick medial motoneurons ($p = 0.94$). Similarly, the average membrane resistance (1100 ± 170) (Fig. 7*Bii*) ($n = 10$) was also not significantly different from the endogenous chick MMC_m neurons ($p = 0.24$). Both the average whole-cell capacitance and membrane resistance of the ES cell-derived motoneurons were significantly different from the endogenous chick lateral motoneurons ($p = 0.04$ and $p \ll 0.001$, respectively). The membrane time constant of the ES cells (i.e., 48 ms) was closer to that of the MMC_m than the LMC neurons. No differences were found in the resting membrane potential of endogenous medial, lateral, or ES cell-derived motoneurons (Fig. 7*Biii*). Together, these data indicate that transplanted ES cell-derived motoneurons develop electrophysiological properties most consistent with a medial motoneuron identity.

Epigenetic factors can regulate the innervation of ES cell-derived motoneurons

The above results indicate that embryoid bodies differentiate into motoneurons that are anatomically and physiologically similar to MMC_m motoneurons when treated with Hh-Ag1.3 and RA. It therefore seems conflicting that a previous study showed that HBG3 $Lhx3^+$ ES cell-derived motoneurons extended $eGFP^+$ axons along all peripheral motor nerve branches, including those that innervated limb muscles, when grafted into the neural tube

of st. 15–17 chick embryos (Wichterle et al., 2002). That is, many of the grafted ES cell-derived motoneurons projected to muscle targets that were inappropriate for their LIM homeodomain code. However, as noted by Wichterle et al. (2002), a similar mismatch between the LIM homeodomain code of motoneurons and axonal trajectories was reported in TgH Lhx3^{on} mouse embryos (Sharma et al., 2000). All motoneurons in TgH Lhx3^{on} mice express Lhx3 and thus develop a MMC_m motoneuron identity. Nonetheless, although axial muscle innervation was substantially increased in TgH Lhx3^{on} mice, many motoneurons still projected into the limb (Sharma et al., 2000). Shunting of axons from heavily occupied axonal targets was suggested as the most plausible explanation for the mistargeting of Lhx3$^+$ motoneurons into the limbs in TgH Lhx3^{on} mice (Sharma et al., 2000). Consequently, Lhx3$^+$ ES cell-derived motor axons could have projected to the limb in Wichterle et al. (2002), because the axial muscle and/or pathway only permitted innervation from a finite number of axons.

To directly test the possibility that an oversupply of ES cell-derived motoneurons could lead to innervation of limb muscles, we transplanted large Shh-Ag1.3/RA-treated embryoid bodies containing ~275 ES cell-derived motoneurons into st. 17 chick embryos. This number of ES cell-derived motoneurons is more than twice that grafted in the transplant experiments described above. The embryos were allowed to develop until st. 31. As observed with smaller embryoid bodies containing 120 eGFP$^+$ cells, the vast majority of the transplanted ES cell-derived motoneurons migrated through the ependymal layer to reside within the medial aspect of the developing spinal cord (Fig. 8*B*, green dots). Furthermore, all of the transplanted eGFP$^+$ motoneurons were Lhx3$^+$ ($n = 3$, data not shown). As shown in Figure 8, many of the eGFP$^+$ axons projected dorsally as part of the dorsal ramus (Fig. 8*A*,*B*, long arrow) where they eventually bifurcated to innervate either the longissimus muscle or skin. However, in contrast to when 120 eGFP$^+$ motoneurons were transplanted, several eGFP$^+$ axons in the large embryoid bodies extended along major peripheral axonal pathways that ultimately led to the limb (Fig. 8*A*,*B*, short arrow) or the ilio-femoralis internus muscle (Fig. 8*A*,*B*, arrowhead). These results support the hypothesis that the genetic program mediating axon targeting in ES cell-derived motoneurons expressing Lhx3 is overridden when the occupancy of the preferred navigational pathway is elevated beyond its maximum capacity.

Could overcrowding of the preferred navigational pathway explain why some eGFP$^+$ motor axons always projected from the dorsal ramus into the skin (Fig. 3)? To directly test this possibility, we transplanted ~10 eGFP$^+$ cells into the ventral neural tube of st. 17 embryos ($n = 3$). Surprisingly, despite the small number of transplanted cells, two to four eGFP$^+$ axons always innervated the longissimus muscle (Fig. 8*C*, arrow), whereas another two to four axons misprojected into the skin (Fig. 8*C*, arrowhead). These results indicate that overcrowding of motor axons in the longissimus nerve cannot explain why cutaneous misprojections occurred, because substantially more than two to four eGFP$^+$ axons innervated the longissimus muscle when 120 cells were transplanted (Fig. 3*D*).

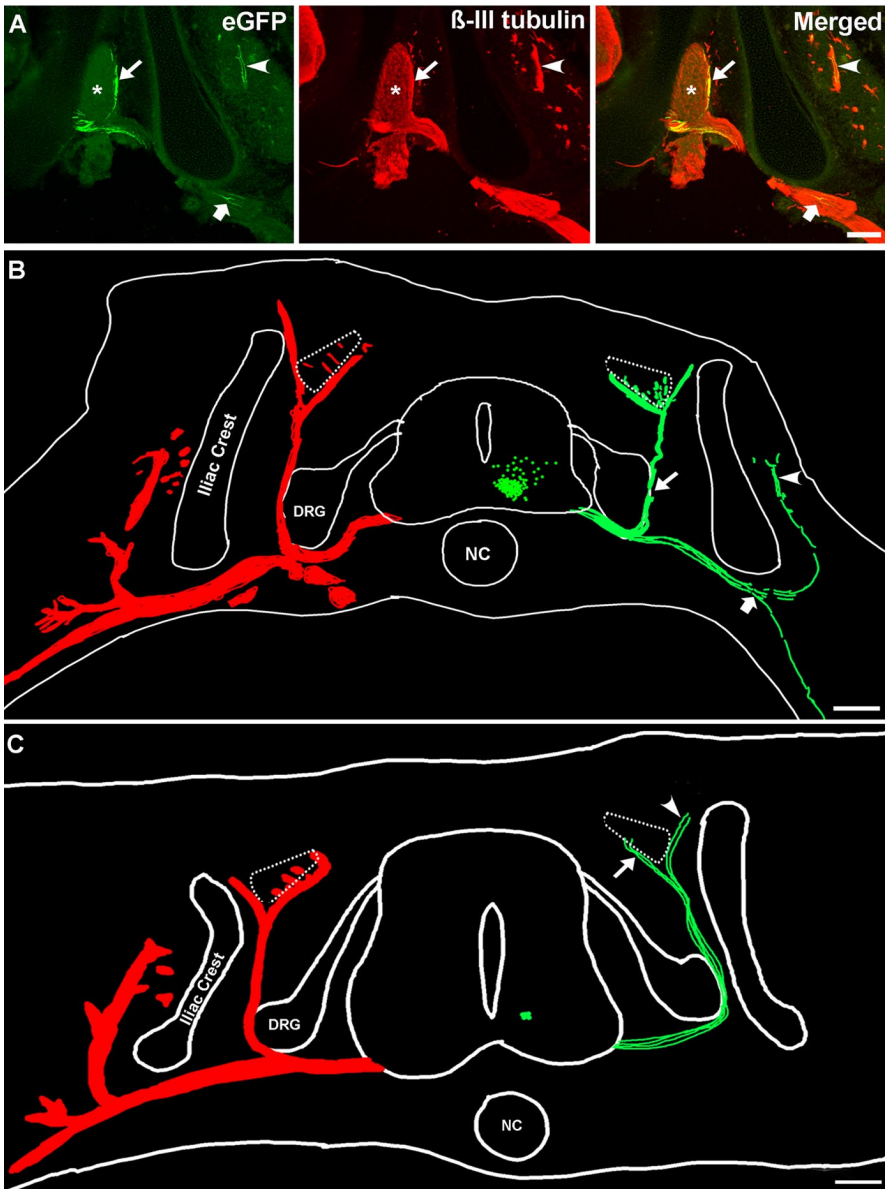

Figure 8. Transplanted ES cell-derived motoneurons can project axons to limb muscles. ***A***, Cross sections through a st. 31 chick embryo transplanted with ~275 ES cell-derived motoneurons cells shows that the eGFP$^+$ axons either projected dorsally along the dorsal ramus (***A***, ***B***, long arrow), or extended along other major peripheral axonal pathways that ultimately led to the ilio-femoralis internus muscle (***A***, ***B***, arrowhead) or into the developing limb (***A***, ***B***, short arrow). ***B***, Neurolucida reconstruction shows all of the eGFP$^+$ motoneurons (green tracings) in a representative st. 31 chick embryo transplanted with ~275 ES cell-derived motoneurons. For comparison, the projection patterns of the endogenous β-III tubulin$^+$ chick neurons are shown in red on the contralateral side. ***C***, Neurolucida reconstruction shows that some eGFP$^+$ motor axons misproject to the skin even when only 10 eGFP$^+$ cells are transplanted into the neural tube. NC, Notochord. Scale bars: ***A***, 20 μm; ***B***, ***C***, 100 μm.

ES cell-derived motoneurons innervating the longissimus muscle express polysialic acid

It is well established that developing motoneurons misproject to inappropriate targets if their axons do not express polysialic acid

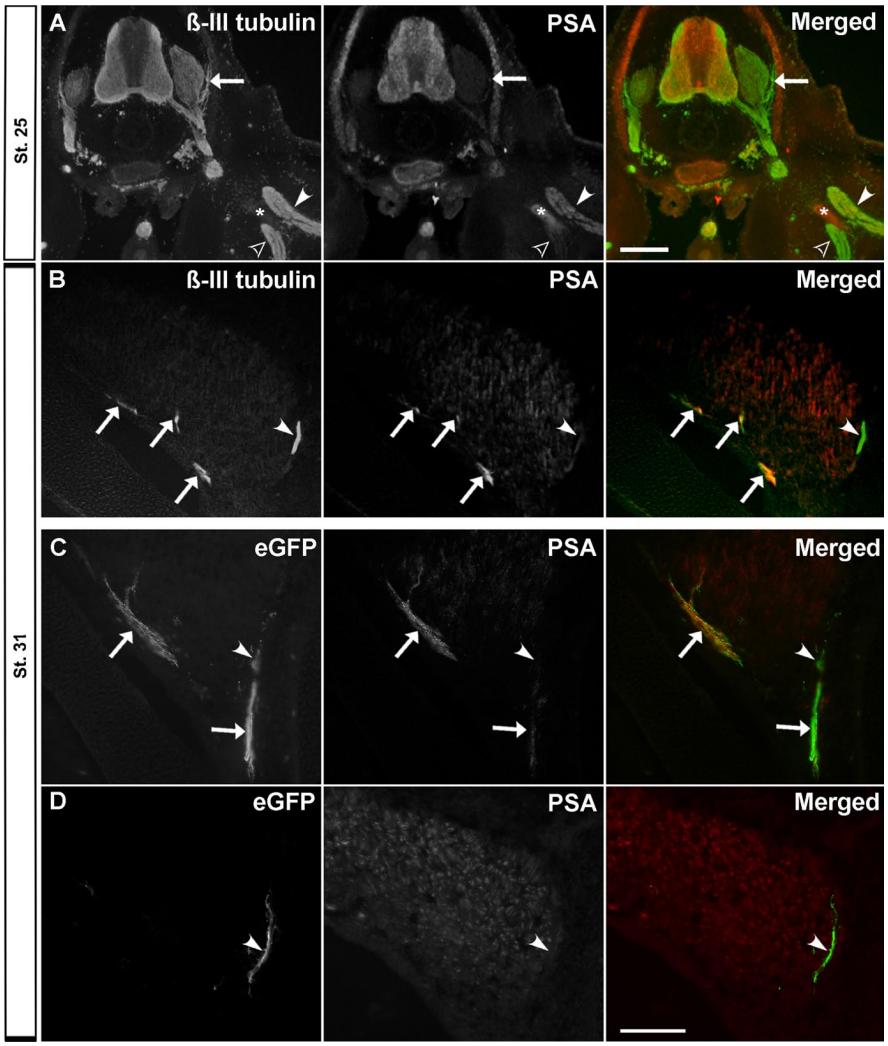

Figure 9. ES cell-derived motor axons projecting to the epaxial muscle and skin differentially express PSA. ***A***, Cross section of a control st. 25 embryo immunostained for β-III tubulin and PSA shows that PSA is not expressed by axons as they form the dorsal ramus (arrow). As expected, the dorsal nerve trunk projecting into the hindlimb expressed more PSA (arrowhead) than the ventral nerve truck (open arrowhead). The asterisk denotes autofluorescing bone. ***B***, At stage 31, the muscle component of the dorsal ramus expresses PSA (arrows), whereas the sensory component does not (arrowhead). ***C***, ***D***, eGFP$^+$ axons projecting to the longissimus muscle express high levels of PSA (arrow), whereas the eGFP$^+$ axons extending to the skin along the cutaneous nerve do not (arrowheads). In all sections, dorsal is up. Scale bars: ***A***, 100 μm; (in ***D***) ***B–D***, 200 μm.

(PSA) (Tang et al., 1992, 1994) (for review, see Landmesser, 2001). Although mistargeting of motor axons to the skin was not examined by Tang et al. (1992, 1994), a recent study by Franz et al. (2005) showed that regenerating motor axons have a higher than normal propensity to grow along cutaneous nerves if they do not express PSA. Inspired by these studies, we investigated whether PSA was differentially expressed by eGFP$^+$ axons innervating the longissimus muscle and skin. Figure 9*A* shows that, although PSA is expressed on the dorsal nerve trunk innervating the hindlimb (arrowhead), it is not expressed by axons in the dorsal ramus (arrow) or ventral nerve trunk (open arrowhead) at st. 25 (Tang et al., 1992). Interestingly, PSA is highly expressed on motor axons when they begin to branch from the dorsal ramus to innervate the longissimus muscle (Fig. 9*B*, arrows) at st. 31. The cutaneous axons expressed little PSA at the same stage in development (Fig. 9*B*, arrowhead). Cross sections through the developing longissimus muscle at st. 31 in transplanted embryos ($n = 3$) showed that eGFP$^+$ axons projecting to the muscle expressed high levels of PSA (Fig. 9*C*, arrows), whereas the eGFP$^+$ axons extending to the skin did not (Fig. 9*C*,*D*, arrowheads). Together with previous studies (Tang et al., 1992, 1994), these results provide correlative evidence that ES cell-derived motoneurons must express PSA to correctly innervate their appropriate muscle target.

Discussion

It is well established that ES cells differentiate into functional motoneurons *in vitro* when treated with a Shh agonist and RA (Wichterle et al., 2002; Harper et al., 2004; Miles et al., 2004; Li et al., 2005). Our present results extend these findings to show that Hh-Ag1.3- and RA-treated ES cells differentiate into motoneurons specific to the MMC_m. Several lines of evidence support this conclusion. First, treated ES cells stably express Lhx3 *in vitro*. Second, transplanted ES cell-derived motoneurons express Lhx3, migrate to the MMC_m, selectively extend neurites to epaxial muscles, and develop electrophysiological properties that are similar to MMC_m motoneurons. These results are important in the development of strategies for cell replacement therapy that are designed to direct ES cells to differentiate into specific neuronal phenotypes, because they demonstrate that neurotransmitter phenotype is insufficient in establishing neuronal identity.

Generation of diverse motoneuronal phenotypes

Motoneurons innervating muscles of similar embryonic origin are highly segregated within columns that are aligned along the medial–lateral axis of the spinal cord (Landmesser, 1978a,b). Motoneurons innervating epaxial muscles adjacent to the vertebrae are located in the MMC_m. Motoneurons innervating limb muscles are located laterally within the LMC. The LMC is subdivided into two additional columns containing motoneurons that innervate muscles derived from the ventral (LMC_m) and dorsal muscle masses (LMC_l). The combinatorial expression of specific LIM homeodomain transcription factors can be used to anatomically identify these discrete columns (Tsuchida et al., 1994). Islet1/2 and Lhx3 expression demarcates the MMC_m, Islet2 and Lim1 delineates the LMC_l, whereas Islet1/2 alone defines motoneurons in the LMC_m. These LIM homeodomain transcription factors are believed to regulate the migration of the motoneurons from the ependymal cell layer to the discrete motor columns and coordinate the outgrowth of their axons to the specific muscle targets (for review, see Jessell, 2000; Landmesser, 2001; Sharma and Belmonte, 2001; Price and Briscoe, 2004).

In this study, we demonstrate that ES cell-derived motoneurons expressed Lhx3 5 d after transplantation. Thus, Lhx3 was expressed from the time the cells were implanted (Wichterle et al., 2002) to the point at which their axons were making neuro-

muscular contact (Fig. 3). The selective migration of the transplanted ES cell-derived motoneurons to the MMC_m (Fig. 2) supports the hypothesis that Lhx3 contributes to the segregation of MMC_m and LMC neurons by limiting the lateral migration of $Lhx3^+$ neurons to the medial aspect of the developing spinal cord (Sharma et al., 1998). The selective projection of axons from the transplanted ES cell-derived motoneurons to the epaxial muscles (Fig. 3) also supports the hypothesis that Lhx3 coordinates the targeting of MMC_m motoneurons (Sharma et al., 2000). The incorrect projection of ES cell-derived motor axons from the dorsal ramus to the skin may be explained by the fact that the misprojecting axons do not express PSA (Fig. 9). PSA is required for proper motor axon guidance during development (Tang et al., 1992, 1994; Rafuse and Landmesser, 2000). Interestingly, Landmesser and colleagues recently showed that motoneurons are spontaneously active before muscle contact (Milner and Landmesser, 1999; Hanson and Landmesser, 2003) and that this activity is required for both proper PSA expression and axon targeting (Hanson and Landmesser, 2004). It is therefore tempting to speculate that the ES cell-derived motoneurons projecting to the longissimus muscle are more active and physiologically integrated within the host nervous system than those projecting to the skin.

At present, it is not known what downstream signals direct MMC_m axons to correctly innervate their appropriate muscle targets during development. However, recent studies indicate that Eph receptor tyrosine kinases and their ephrin ligands are likely involved in this selective axon guidance process (Eberhart et al., 2004). EphA4 is expressed by MMC_m axons as they sort out in the plexus region where they later project dorsally as part of the dorsal ramus (Helmbacher et al., 2000; Kania and Jessell, 2003; Eberhart et al., 2004). Its ephrin-A5 ligand is localized in the rostral half-sclerotome through which the dorsal projecting MMC_m pass en route to the developing axial muscles (Eberhart et al., 2004). Although ephrin-A5 is inhibitory for $EphA4^+$ motor axons that project to the dorsal muscle mass in the limbs (Eberhart et al., 2002; Kania and Jessell, 2003), it exerts positive effects on $EphA4^+$ MMC_m motor axons innervating epaxial muscles (Eberhart et al., 2004). Thus, like MMC_m neurons, ES cell-derived motoneurons may selectively target epaxial muscles because their axons express EphA4 (Fig. 5) that facilitates growth through the ephrin-$A5^+$ sclerotome.

However, EphA4/ephrinA5 interactions cannot fully account for the selective targeting of the endogenous MMC_m neurons or transplanted ES cell-derived motoneurons. Previous studies in chick (Tosney, 1987; Tosney and Hageman, 1989) and mouse (Kablar and Rudnicki, 1999) embryos showed that the motor component of the dorsal ramus does not develop if the axial muscles are prevented from forming. Thus, chemotropic signals from the developing dermamyotome and/or muscle may selectively guide MMC_m motoneurons (Tosney, 1987). In the present study, $Lhx3^+$ ES cell-derived motoneurons selectively targeted epaxial muscles even when they were ectopically transplanted into the dorsal one-half of the neural tube or when flanked by longissimus and caudilioflexorius muscle fibers *in vitro* (Fig. 6). Thus, like MMC_m neurons, ES cell-derived motoneurons may selectively target epaxial muscles, because the target secretes a diffusible chemotropic factor that is specific for $Lhx3^+$ axons.

The electrophysiological studies of the transplanted cells not only demonstrated that they developed the appropriate machinery to function as motoneurons, such as firing repetitively, but also that they can receive synaptic input *in vivo*. Furthermore, the passive properties of these neurons were similar to those of endogenous MMC_m motoneurons. Although these properties alone cannot be used to define MMC_m motoneurons, and may primarily reflect the properties seen in smaller motoneurons (Zengel et al., 1985), together with the anatomical data presented above, these data support the concept that the ES cell-derived motoneurons assume a MMC_m identity. Whether the transplanted ES cell-derived motoneurons are physiologically integrated within the host nervous system, and activated like epaxial motoneurons during motor activity is presently not known. This question ultimately will have to be resolved if cell replacement therapy is to become a viable treatment strategy for neurodegenerative diseases.

Implications for cell replacement therapy

Several studies have shown that ES cells can be directed to differentiate into electrically excitable glutamatergic (Plachta et al., 2004), serotonergic (Lee et al., 2000), dopaminergic (Kim et al., 2002), or cholinergic motor (Wichterle et al., 2002; Harper et al., 2004; Miles et al., 2004; Li et al., 2005) neurons. However, differentiated ES cells will ultimately have to be classified by other means, because subpopulations of neurons that express a given transmitter can differ dramatically with respect to size, ion channels, receptors, projection patterns, and, most importantly, function. Furthermore, several neurodegenerative disorders result in the selective loss of specific neuronal subtypes. For example, dopamine neurons expressing the G-protein-coupled inward rectifying current potassium channel (Girk2) preferentially degenerate in patients with PD (Yamada et al., 1990; Fearnley and Lees, 1991; Gibb, 1992; Mendez et al., 2005). Enkephalin-containing GABAergic neurons projecting from the striatum to the external segment of the globus pallidus are the first to degenerate in patients with Huntington's disease (Reiner et al., 1988; Sapp et al., 1995). The fastest conducting, and presumably largest, motor neurons preferentially die in patients with amyotrophic lateral sclerosis (Theys et al., 1999).

One of the guiding assumptions underlying cell replacement therapy is that the transplanted neurons will form selective connections with the appropriate target tissue. Whether this assumption is correct is not known. However, there are now several lines of evidence to suggest that specific connections do occur between transplant and host neurons. For example, fetal ventral mesencephalic tissue, used in the treatment of animal models of PD, contains a mixture of two dopamine neuron subtypes: A9 ($Girk2^+$) neurons of the substantia nigra that project to the striatum and A10 neurons of the ventral tegmental area. Interestingly, only A9 neurons extend axons out of the graft when the tissue is transplanted into the striatum of animal models of PD (Thompson et al., 2005), and in humans with the disease (Mendez et al., 2005). These results suggest that many of the guidance molecules and/or trophic factors expressed during development exist in the adult CNS. They also underscore the fact that neuronal specificity is required for optimal growth and synapse formation (Thompson et al., 2005) (for review, see Bjorklund and Isacson, 2002). Thus, it may not be sufficient to simply generate generic neurons from ES cells, or even neurons of a particular transmitter phenotype, when treating diseases or trauma. Specific neuronal subpopulations that provide for the particular needs of the affected CNS will ultimately have to be developed. With respect to cell replacement therapy and the treatment of spinal cord pathologies, our results imply that limb innervation will be greater if ES cells are differentiated into LMC motoneurons. Although it is not known how to differentiate ES cells into LMC neurons, this process will likely require additional instructive signals that normally emanate from the developing spinal cord (Sockanathan and Jessell, 1998).

References

Abercrombie M (1946) Estimation of nuclear population from microtome sections. Anat Neurobiol Rec 94:239–247.

Bjorklund LM, Isacson O (2002) Regulation of dopamine cell type and transmitter function in fetal and stem cell transplantation for Parkinson's disease. Prog Brain Res 138:411–420.

Chisholm A, Tessier-Lavigne M (1999) Conservation and divergence of axon guidance mechanisms. Curr Opin Neurobiol 9:603–615.

Dahm LM, Landmesser LT (1991) The regulation of synaptogenesis during normal development and following activity blockade. J Neurosci 11:238–255.

Dasen JS, Tice BC, Brenner-Morton S, Jessell TM (2005) A hox regulatory network establishes motor neuron pool identity and target-muscle connectivity. Cell 123:477–491.

Eberhart J, Swartz ME, Koblar SA, Pasquale EB, Krull CE (2002) EphA4 constitutes a population-specific guidance cue for motor neurons. Dev Biol 247:89–101.

Eberhart J, Barr J, O'Connell S, Flagg A, Swartz ME, Cramer KS, Tosney KW, Pasquale EB, Krull CE (2004) Ephrin-A5 exerts positive or inhibitory effects on distinct subsets of EphA4-positive motor neurons. J Neurosci 24:1070–1078.

Ericson J, Briscoe J, Rashbass P, van Heyningen V, Jessell TM (1997a) Graded sonic hedgehog signaling and the specification of cell fate in the ventral neural tube. Cold Spring Harb Symp Quant Biol 62:451–466.

Ericson J, Rashbass P, Schedl A, Brenner-Morton S, Kawakami A, van Heyningen V, Jessell TM, Briscoe J (1997b) Pax6 controls progenitor cell identity and neuronal fate in response to graded Shh signaling. Cell 90:169–180.

Fearnley JM, Lees AJ (1991) Ageing and Parkinson's disease: substantia nigra regional selectivity. Brain 114:2283–2301.

Franz CK, Rutishauser U, Rafuse VF (2005) Polysialylated neural cell adhesion molecule is necessary for selective targeting of regenerating motor neurons. J Neurosci 25:2081–2091.

Gibb WR (1992) Melanin, tyrosine hydroxylase, calbindin and substance P in the human midbrain and substantia nigra in relation to nigrostriatal projections and differential neuronal susceptibility in Parkinson's disease. Brain Res 581:283–291.

Guthrie S, Lumsden A (1994) Collagen gel coculture of neural tissue. Neuroprotocols 4:116–120.

Hamburger V (1958) Regression versus peripheral control of differentiation in motor hypoplasia. Am J Anat 102:365–410.

Hamburger V (1975) Cell death in the development of the lateral motor column of the chick embryo. J Comp Neurol 160:535–546.

Hamburger V, Hamilton HL (1951) A series of normal stages in the development of the chick embryo. J Morphol 88:49–82.

Hanson MG, Landmesser LT (2003) Characterization of the circuits that generate spontaneous episodes of activity in the early embryonic mouse spinal cord. J Neurosci 23:587–600.

Hanson MG, Landmesser LT (2004) Normal patterns of spontaneous activity are required for correct motor axon guidance and the expression of specific guidance molecules. Neuron 43:687–701.

Harper JM, Krishnan C, Darman JS, Deshpande DM, Peck S, Shats I, Backovic S, Rothstein JD, Kerr DA (2004) Axonal growth of embryonic stem cell-derived motoneurons in vitro and in motoneuron-injured adult rats. Proc Natl Acad Sci USA 101:7123–7128.

Helmbacher F, Schneider-Maunoury S, Topilko P, Tiret L, Charnay P (2000) Targeting of the EphA4 tyrosine kinase receptor affects dorsal/ventral pathfinding of limb motor axons. Development 127:3313–3324.

Hollyday M, Hamburger V (1977) An autoradiographic study of the formation of the lateral motor column in the chick embryo. Brain Res 132:197–208.

Jessell T (2000) Neuronal specification in the spinal cord: inductive signals and transcriptional codes. Nat Rev Genet 1:20–29.

Kablar B, Rudnicki MA (1999) Development in the absence of skeletal muscle results in the sequential ablation of motor neurons from the spinal cord to the brain. Dev Biol 208:93–109.

Kania A, Jessell TM (2003) Topographic motor projections in the limb imposed by LIM homeodomain protein regulation of ephrin-A:EphA interactions. Neuron 38:581–596.

Kania A, Johnson RL, Jessell TM (2000) Coordinate roles for LIM homeobox genes in directing the dorsoventral trajectory of motor axons in the vertebrate limb. Cell 102:161–173.

Keller G (2005) Embryonic stem cell differentiation: emergence of a new era in biology and medicine. Genes Dev 19:1129–1155.

Kim JH, Auerbach JM, Rodríguez-Gómez JA, Velasco I, Gavin D, Lumelsky N, Lee S-H, Nguyen J, Sánchez-Pernaute R, Bankiewicz K, McKay R (2002) Dopamine neurons derived from embryonic stem cells function in an animal model of Parkinson's disease. Nature 418:50–56.

Landmesser L (1978a) The distribution of motoneurones supplying chick hind limb muscles. J Physiol (Lond) 284:371–389.

Landmesser L (1978b) The development of motor projection patterns in the chick hind limb. J Physiol (Lond) 284:391–414.

Landmesser L (2001) The acquisition of motoneuron subtype identity and motor circuit formation. Int J Dev Neurosci 19:175–182.

Landmesser LT (1992) Growth cone guidance in the avian limb: a search for cellular and molecular mechanisms. In: The nerve growth cone (Letourneau PC, Kater SB, Macagno ER, eds), pp 373–385. New York: Raven.

Lee S-H, Lumelsky N, Studer L, Auerbach JM, McKay RD (2000) Efficient generation of midbrain and hindbrain neurons from mouse embryonic stem cells. Nat Biotech 18:675–679.

Li XJ, Du ZW, Zarnowska ED, Pankratz M, Hansen LO, Pearce RA, Zhang SC (2005) Specification of motoneurons from human embryonic stem cells. Nat Biotechnol 23:215–221.

Lupa MT, Hall ZW (1989) Progressive restriction of synaptic vesicle protein to the nerve terminal during development of the neuromuscular junction. J Neurosci 9:3937–3945.

Martin I, Dozin B, Quarto R, Cancedda R, Beltrame F (1997) Computer-based technique for cell aggregation analysis and cell aggregation in *in vitro* chondrogenesis. Cytometry 28:141–146.

Mendez I, Sanchez-Pernaute R, Cooper O, Vinuela A, Ferrari D, Bjorklund L, Dagher A, Isacson O (2005) Cell type analysis of functional fetal dopamine cell suspension transplants in the striatum and substantia nigra of patients with Parkinson's disease. Brain 128:1498–1510.

Miles GB, Yohn DC, Wichterle H, Jessell TM, Rafuse VF, Brownstone RM (2004) Functional properties of motoneurons derived from mouse embryonic stem cells. J Neurosci 24:7848–7858.

Milner LD, Landmesser LT (1999) Cholinergic and GABAergic inputs drive patterned spontaneous motoneuron activity before target contact. J Neurosci 19:3007–3022.

Oppenheim RW, Chu-Wang IW, Maderdrut JL (1978) Cell death of motoneurons in the chick embryo spinal cord. III. The differentiation of motoneurons prior to their induced degeneration following limb-bud removal. J Comp Neurol 177:87–111.

Plachta N, Bibel M, Tucker KL, Barde YA (2004) Developmental potential of defined neural progenitors derived from mouse embryonic stem cells. Development 131:5449–5456.

Price SR, Briscoe J (2004) The generation and diversification of spinal motor neurons: signals and responses. Mech Devel 121:1103–1115.

Rafuse VF, Landmesser LT (2000) The pattern of avian intramuscular nerve branching is determined by the innervating motoneuron and its level of polysialic acid. J Neurosci 20:1056–1065.

Reiner A, Albin RL, Anderson KD, D'Amato CJ, Penney JB, Young AB (1988) Differential loss of striatal projection neurons in Huntington disease. Proc Natl Acad Sci USA 85:5733–5737.

Sapp E, Ge P, Aizawa H, Bird E, Penney J, Young AB, Vonsattel JP, DiFiglia M (1995) Evidence for a preferential loss of enkephalin immunoreactivity in the external globus pallidus in low grade Huntington's disease using high resolution image analysis. Neuroscience 64:397–404.

Sharma K, Belmonte JC (2001) Development of the limb neuromuscular system. Curr Opin Cell Biol 13:204–210.

Sharma K, Sheng HZ, Lettieri K, Li H, Karavanov A, Potter S, Westphal H, Pfaff SL (1998) LIM homeodomain factors Lhx3 and Lhx4 assign subtype identities for motor neurons. Cell 95:817–828.

Sharma K, Leonard AE, Lettieri K, Pfaff SL (2000) Genetic and epigenetic mechanisms contribute to motor neuron pathfinding. Nature 406:515–519.

Sockanathan S, Jessell TM (1998) Motor neuron-derived retinoid signaling specifies the subtype identity of spinal motor neurons. Cell 94:503–514.

Tanaka H, Landmesser LT (1986) Cell death of lumbosacral motoneurons in chick, quail, and chick-quail chimera embryos: a test of the quantitative matching hypothesis of neuronal cell death. J Neurosci 6:2889–2899.

Tang J, Landmesser L, Rutishauser U (1992) Polysialic acid influences specific pathfinding by avian motoneurons. Neuron 8:1031–1044.

Tang J, Landmesser L, Rutishauser U (1994) Polysialic acid regulates growth

cone behavior during sorting of motor axons in the plexus region. Neuron 13:405–414.

Tessier-Lavigne M, Goodman CS (1996) The molecular biology of axon guidance. Science 274:1123–1133.

Theys PA, Peeters E, Robberecht W (1999) Evolution of motor and sensory deficits in amyotrophic lateral sclerosis estimated by neurophysiological techniques. J Neurol 246:438–442.

Thompson L, Barraud P, Andersson E, Kirik D, Bjorklund A (2005) Identification of dopaminergic neurons of nigral and ventral tegmental area subtypes in grafts of fetal ventral mesencephalon based on cell morphology, protein expression, and efferent projections. J Neurosci 25:6467–6477.

Tosney KW (1987) Proximal tissues and patterned neurite outgrowth at the lumbosacral level of the chick embryo: deletion of the dermamyotome. Dev Biol 122:540–558.

Tosney KW, Hageman MS (1989) Different subsets of axonal guidance cues are essential for sensory neurite outgrowth to cutaneous and muscle targets in the dorsal ramus of the embryonic chick. J Comp Neurol 251:232–244.

Tosney KW, Landmesser LT (1985a) Development of the major pathways for neurite outgrowth in the chick hindlimb. Dev Biol 109:193–214.

Tosney KW, Landmesser LT (1985b) Growth cone morphology and trajectory in the lumbosacral region of the chick embryo. J Neurosci 5:2345–2358.

Tsuchida T, Ensini M, Morton SB, Baldassare M, Edlund T, Jessell TM, Pfaff SL (1994) Topographic organization of embryonic motor neurons defined by expression of LIM homeobox genes. Cell 79:957–970.

Wichterle H, Lieberam I, Porter JA, Jessell TM (2002) Directed differentiation of embryonic stem cells into motor neurons. Cell 110:385–397.

Yamada T, McGeer PL, Baimbridge KG, McGeer EG (1990) Relative sparing in Parkinson's disease of substantia nigra dopamine neurons containing calbindin-D28K. Brain Res 526:303–307.

Zengel JE, Reid SA, Sypert GW, Munson JB (1985) Membrane electrical properties and prediction of motor-unit type of medial gastrocnemius motoneurons in the cat. J Neurophysiol 53:1323–1344.